International Journal of Pharmaceutics 390 (2010) 214–224

Contents lists available at ScienceDirect

International Journal of Pharmaceutics

journal homepage: www.elsevier.com/locate/ijpharm

Pharmaceutical Nanotechnology

# Cell-specific targeting in the mouse inner ear using nanoparticles conjugated with a neurotrophin-derived peptide ligand: Potential tool for drug delivery

Soumen Roy[a], Alex H. Johnston[c], Tracey A. Newman[c], Rudolf Glueckert[a,b], Jozsef Dudas[a], Mario Bitsche[a], Elisa Corbacella[d], Gunde Rieger[a], Alessandro Martini[d], Anneliese Schrott-Fischer[a,*]

[a] Department of Otolaryngology, Medical University of Innsbruck, Anichstr. 35, A-6020 Innsbruck, Austria
[b] University Clinics of Innsbruck, Tiroler Landeskrankenanstalten GmbH-TILAK, A-6020 Innsbruck, Austria
[c] School of Biological Sciences, University of Southampton, Southampton, SO16 7PX, United Kingdom
[d] Department of Audiology, University of Ferrara, 44100 Ferrara, Italy

ARTICLE INFO

*Article history:*
Received 25 November 2009
Received in revised form 3 February 2010
Accepted 4 February 2010
Available online 11 February 2010

*Keywords:*
Inner ear
Spiral ganglion neurons
Nanoparticles
Hearing loss

ABSTRACT

Cell specific targeting is an emerging field in nanomedicine. Homing of the multifunctional nanoparticles (MFNPs) is achieved by the conjugation of targeting moieties on the nanoparticle surface. The inner ear is an attractive target for new drug delivery strategies as it is hard to access and hearing loss is a significant worldwide problem. In this work we investigated the utility of a Nerve Growth Factor-derived peptide (hNgf_EE) functionalized nanoparticles (NPs) to target cells of the inner ear. These functionalized NPs were introduced to organotypic explant cultures of the mouse inner ear and to PC-12 rat pheochromocytoma cells. The NPs did not show any signs of toxicity. Specific targeting and higher binding affinity to spiral ganglion neurons, Schwann cells and nerve fibers of the explant cultures were achieved through ligand mediated multivalent binding to tyrosine kinase receptors and to p75 neurotrophin receptors. Unspecific uptake of NPs was investigated using NPs conjugated with scrambled hNgf_EE peptide. Our results indicate a selective cochlear cell targeting by MFNPs, which may be a potential tool for cell specific drug and gene delivery to the inner ear.



## 1. Introduction

One of the current initiatives in medicine is the exploitation of nanosized drug delivery vehicles, nanoparticles (NPs) to complement existing therapeutic strategies (Farokhzad and Langer, 2006; Malam et al., 2009). NP mediated drug delivery may offer increased efficacy and reduced drug-associated side effects. The increased efficacy will occur in part as a consequence of the ability to target the drug, within the NP, to the site within the tissue where the therapeutic effect is required (Gelperina et al., 2005). Entrapment of the drug within the NP and controlled release at the required site may result in lower doses of drugs needed and hence reduced side effects. Targeting of the NPs require the identification of suitable ligands to receptors which are selectively expressed at higher levels within the target tissue. Inner ear disease is a significant worldwide problem, with hearing loss affecting as many as 44 million people within the European Union alone. Strategies to prevent hearing loss are limited, and the cochlea is difficult to access by conventional systemic drug delivery due to the presence of the cochlea-blood barrier.

Neurotrophins are secreted growth factors and plays an important role for the survival, development, maintenance of neurons in both the peripheral and central nervous systems of vertebrates (Huang and Reichardt, 2001, 2003; He and Garcia, 2004; Reichardt, 2006). The neurotrophin family, including nerve growth factor, brain-derived neurotrophic factor, neurotrophin-3 and neurotrophin 4/5, signals through two distinct groups of cell surface receptors the Trks (Tyrosine kinase receptors) and p75 neurotrophin receptor (Kaplan and Miller, 1997, 2000). Neurotrophins and their receptors are reported to regulate the survival of vestibular and cochlear neurons (Fritzsch et al., 1997, 2006). In this study we investigated the targeting of polymersome NPs to cells of the inner ear by conjugation of neurotrophin-derived peptides.

Amphiphilic block copolymers, consisting of chains of hydrophobic and hydrophilic units, self-assemble into polymersome NPs (Fig. 1) in an aqueous environment (Letchford and Burt, 2007). Structurally polymersomes are similar to liposomes, however, they have several advantages over liposomes, which give them greater potential as drug delivery vehicles. The membrane thickness can be controlled by the molecular weight of the hydrophobic block copolymer, to achieve thicker, stronger membranes making them more stable than conventional

* Corresponding author at: Department of Otolaryngology, Medical University of Innsbruck, Inner Ear Research Laboratory, Anichstr. 35, 6020 Innsbruck, Austria. Tel.: +43 512 504 23176; fax: +43 512 504 23175.
*E-mail address:* annelies.schrott@i-med.ac.at (A. Schrott-Fischer).

0378-5173/$ – see front matter © 2010 Elsevier B.V. All rights reserved.
doi:10.1016/j.ijpharm.2010.02.003

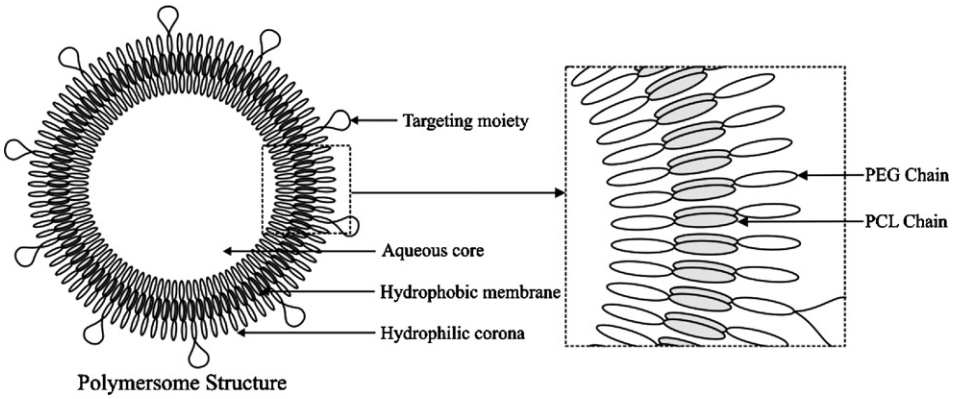


**Fig. 1.** PEG-*b*-PCL block copolymers (PEG – polyethylene glycol and PCL – polycaprolactone) self-assemble in an aqueous environment to form polymersome structures. The PCL units of the polymer form a hydrophobic membrane. The PEG units form a hydrophilic corona and line the interior cavity of the polymersome. The surface can be functionalized with targeting moieties.

liposomes (Discher et al., 1999). Small molecular weight hydrophobic molecules can be incorporated into the membrane (Lin et al., 2006). The polymersome surface can be functionalized with groups to promote cellular uptake (Christian et al., 2007). Targeting ligands such as short peptide sequences, derived from human nerve growth factor (hNGF) beta, can be conjugated to the end of the hydrophilic segment so that they may extend outward from the nanoparticle corona. The targeting ligands then readily encounter and interact with membrane surface receptors Trks and p75 neurotrophin receptor.

The main purpose of functionalization of the hydrophilic corona is to modulate biodistribution of polymeric NPs and induce cellular uptake by receptor-mediated endocytosis (Mukherjee et al., 1997; Lindgren et al., 2000). Targeted uptake of multifunctional nanoparticles in a cell, tissue or disease specific manner represents a potentially powerful technology in biomedicine (Farokhzad et al., 2006a,b).

In this study we focused on binding of peptide-tagged NPs in *in vitro* and *ex vivo* model systems. Confocal laser scanning microscopical analysis demonstrated a high level of selective uptake and specific binding of ligand-conjugated NPs in sensory hair cells, spiral ganglion neurons (SGNs), Schwann cells and along the nerve fibers. In contrast, a low level of non-specific uptake was observed with control NPs conjugated with scrambled peptide sequences of the targeting hNgf_EE peptide.

## 2. Materials and methods

### 2.1. Polymersome preparation

Anhydrous N,N-dimethylformamide (DMF), poly(ethylene glycol)-block-poly($\varepsilon$-caprolactone) methyl ether, PEG average Mn ~5000, and PCL average Mn ~5000 (PEG5K-b-PCL5K), 4-(N-Maleimidomethyl) cyclohexane-1-carboxylic acid 3-sulfo-N-hydroxysuccinimide ester sodium salt (sulfo-SMCC) and glycine were purchased from Sigma–Aldrich (UK). Poly(ethylene glycol)-block-poly($\varepsilon$-caprolactone) methyl ether, PEG average Mn ~5800, PCL average Mn ~19,000, (NH2-PEG5.8K-b-PCL19K) was supplied by Polymer Source Inc. (US). hNgf_EE peptide sequence (CTFVKALTMDGKQAAWR, M.W.: 1926.3) and scrambled hNgf_EE sequence (CWVLTGFTADRAKQMKA, M.W.: 1926.3) was synthesized by Activotec, UK. The scrambled hNgf_EE has the same molecular weight and charge compared to the targeting hNgf_EE peptide. 1,1′-Dioctadecyl-3,3,3′,3′-tetramethyl-indocarbocyanine perchlorate (DiI) was sourced from Invitrogen (UK). The peptide (hNgf_EE) under SEQ ID No. 15 (according to patent WO/2007/051477), TFVKALTMDGKQAAWR, is derived from NGF. The peptide has been shown to bind Trk B (KD = $1 \times 10(-8)$ M), Trk C (KD = $7 \times 10(-8)$ M) and p75 (KD = $2 \times 10(-7)$ M). (Data were obtained by personal communication from Prof. Vladimir Berezin, Protein Laboratory, Department of Neuroscience and Pharmacology, Faculty of Health Sciences, University of Copenhagen N, DK-2200 Copenhagen, Denmark.) Phosphate-buffered saline (PBS) was prepared from phosphate-buffered saline tablets (Oxoid, UK) dissolved in $H_2O$ (purified using a Milli-Q Ultrapure Water Purification System [resistance of 18.2 MΩ cm at 25 °C]). Dialysis tubing with a 12–14 kDa cutoff and 6.3 mm diameter was supplied from Medicell International Ltd. (London, UK). Dynamic light scattering (DLS) was used to measure hydrodynamic radius. 100 μL of sample was diluted with $H_2O$ (4.00 mL). The solution was filtered into a cuvette through a 0.45 μm cellulose acetate membrane. The sample was measured at room temperature; the light was detected at 90°. Data was collected for 30 s and repeated 6 times, the size reported was the average value with the standard deviation. The sample was run on a Coulter N4 Plus particle sizer (Coulter, Fullerton, Ca, USA) using N4 Plus Version 1.10 software for data analysis.

In this study DiI was incorporated into the hydrophobic membrane of the polymersomes, which is a hydrophobic cyanine fluorophore. DiI was used as a fluorescent tracker to observe the distribution of the polymersomes *in vitro* and *ex vivo*.

#### 2.1.1. Unfunctionalized NPs

A 0.1 mg/mL DiI solution in DMF was prepared. PEG5K-b-PCL5K (6 mg) was dissolved into 0.4 mL of the DMF solution and added dropwise (~1 drop every 8 s) to rapidly stirring PBS (1.60 mL). The sample was dialyzed for 48 h against PBS with regular changes of the buffer solution.

#### 2.1.2. hNgf_EE functionalized NPs

A hetero bifunctional linking group can be used to attach cystine containing short chain peptide sequences. A 0.1 mg/mL solution of DiI in DMF was first prepared. PEG5K-b-PCL5K (6.0 mg) and NH2-PEG5.8K-b-PCL19K (6.0 mg) were dissolved in the DMF/DiI solution (0.8 mL). This was added dropwise (~1 drop every 8 s) to stirring PBS (2.40 mL). Sulfo-SMCC (0.5 mg) was dissolved in PBS (0.4 mL), added to the NP solution and stirred for 1 h. Glycine (0.5 mg) was dissolved in PBS (0.4 mL), added to the NP solution and stirred for 15 min. The solution was split into two 2 mL samples. hNgf_EE peptide (CTFVKALTMDGKQAAWR) (1.0 mg) was dissolved in DMF (0.2 mL) and added to one of the 2 mL of NP solution, scrambled hNgf_EE peptide (CWVLTGFTADRAKQMKA) (1.0 mg) was added to the other 2 mL of NP solution. Both samples were stirred overnight then dialyzed for 48 h against PBS with regular changes of the buffer solution, any unbound peptide was removed during dialysis.

In this study the cell uptake and distribution of polymersome nanoparticles made from PEG-*b*-PCL block copolymers functionalized with the hNgf_EE was evaluated in *ex vivo* mouse organotypic cochlea explants. The polymersomes are formed by slow addition of a PEG-*b*-PCL solution in DMF to PBS. A PEG-*b*-PCL polymer with an amine group at the terminus of the PEG unit allows the surface to be functionalized with the hNgf_EE peptide sequence using a sulfo-SMCC hetero-bifunctional linking group.

To allow a greater degree of objectivity when analysing the results from the studies with the organotypic cultures and the PC-12 cells the experiments were performed blinded. The polymersome samples were supplied with codes that did not indicate whether they were functionalized with the hNgf_EE peptide, the scrambled hNgf_EE peptide or no peptide.

#### 2.1.3. Visualization of polymersomes in transmission electron microscopy (TEM)

For particle visualization using TEM the polymersome samples were diluted at 1:50 in Milli-Q water. 1 μL of sample was deposited onto a copper grid coated with formvar and carbon and left to air dry. The slide was negatively stained with 10 μL of 2% uranyl acetate solution; this was applied for 10 s before being blotted off and left to air dry.

### 2.2. Flow cytometry viability assay with pheochromocytoma (PC12) cell cultures

We used two approaches to investigate the potential cytotoxicity as a consequence of exposure to NPs. Firstly, a qualitative evaluation; PC-12 cells were labelled with propidium iodide (PI) to assess plasma membrane integrity. Secondly, we have performed a microscopical analysis of cell morphology. Cell viability was assessed using flow cytometry assays to quantify the fluorescence intensity and, consequently, to discriminate between sub-populations of healthy, dead or apoptosis-approaching cells. A minimum of $1 \times 10^5$ cells were assayed per sample. Flow cytometry analysed the whole population of cells (attached and in suspension), while the microscopy assay only analysed attached cells. Flow cytometry was used to test the NPs safety range.

#### 2.2.1. FACS analysis

PI and all other common laboratory reagents were obtained from Sigma Chemical Co. (St. Louis, MO, USA). Dulbecco's Modified Eagle Medium (DMEM, Gibco), Fetal Bovine Serum (FBS), Normal Horse Serum (NHS), Penicillin–Streptomycine (P/S)-mixture and L-Glutamine (L-glut) were from Gibco, BRL (Grand Island, NY, USA).

The PC-12 (CRL-1721) cell line, obtained from "Istituto Nazionale per la Ricerca sul Cancro" (ISTGE, Genova, Italy), was routinely maintained in DMEM High Glucose (4.5 g/L glucose) supplemented with 10% FBS and 5% NHS, at a density ranging from 0.3 to $1.5 \times 10^6$ cells/mL.

#### 2.2.2. Flow cytometry

Cells were seeded at the density of $7.5 \times 10^5$/mL of fresh culture medium in 6 well plates, after 24 h of incubation (37 °C, 5% $CO_2$) they were treated with NPs at different concentrations. Four dilutions were made of the stock solution (2.5 mg/mL) in order to obtain 25, 12.5, 6.25, 3.125 μg/mL. Non-treated samples were left as a control. After NP exposure, cells were blocked as following: for each sample the medium was drawn away and put in 5 mL polystyrene round-bottom tubes. The cells were trypsinized (500 μL) and resuspended in DMEM and stained with PI. After staining cells were analysed by flow cytometry on a Becton Dickinson FACS-calibur (Becton Dickinson, St. Jose, CA, USA). Untreated cells were used as a reference. The positive control of PI-staining were cells permeabilized by adding Nonidet P40 (0.05% final concentration), stained with PI and analysed.

#### 2.2.3. Fluorescence microscope viability assay

For all the experiments, cells were seeded in 6 well plates at the density of $1.5 \times 10^5$/mL. After 24 h of incubation they were treated with NPs using the same concentrations described above. Cells were incubated (37 °C, 5% $CO_2$) with NPs for 24 h. Cell viability was determined using a PI exclusion assay. At the end of the incubation period PI was added at a final concentration of 50 μg/mL, the samples were allowed to stand for 15 min at room temperature then analysed with a Nikon inverted fluorescence microscope with phase contrast lenses (Nikon, Eclipse TE2000-U, Japan). Cell toxicity was defined estimating the percentage of PI-positive cells in the samples. For each sample digital photomicrographs were obtained using phase contrast for total cells and PI filter for dead cells. Both, viable and dead cells were counted. The toxic effects of the NPs were tested visualizing the ratio between viable cells in samples treated with NPs funtionalized with hNgf_EE or scrambled hNgf_EE peptides.

Analyses of variance (ANOVA) were used to determine the toxic effect of NPs. A Tukey–Kramer multiple comparison test was used to assess statistical significance in the fluorescence microscope viability assay. In the procedure, $p < 0.05$ was the value of statistical significance.

### 2.3. Organotypic culture

Organotypic explant cultures were prepared from mouse cochleae, this represents a complex multi-cellular *in vitro* environment (Sundstrom et al., 2005). We followed an organotypic culture protocol similar to that described previously (Ding et al., 2007). In brief, C57BL/6N mice were sacrificed at post-natal days 1–3 (P1–P3). The cochleae were carefully removed from the skull and microdissection was done in ice cold Hank's Balanced salt solution under Zeiss SteReo Lumar V12 microscope. The stria vascularis and spiral ligament was removed, the organ of Corti with SGNs was cut into apical, middle and basal turn. The tissue was placed onto ice cooled culture dishes (ibidi 60 μDish®) (Nr. 80131, Integrated BioDiagnostics, Martinsried, Germany) on a drop of type I rat tail collagen (BD Biosciences, Vienna, Austria) solution with 10× BME (Sigma) and 2% sodium carbonate. The collagen was allowed to polymerize for approximately 15 min and 1 mL of neurobasal media (Gibco-Invitrogen, Karlsruhe, Germany), B27 supplement (Invitrogen) minus antioxidant, 2 mM glutamine (Gibco), 10 mM HEPES buffer (Gibco) and 100 U/mL penicillin (Sigma, Vienna, Austria). After 4 h of pre-incubation the culture media was replaced with media containing NPs, then incubated further for 12 and 24 h. One dilution was made of the stock solution (2.5 mg/mL) in order to obtain 125 μg/mL. Control samples, containing only media, were run concurrently with the experimental samples and also were incubated for 2 h, 4 h in an another set of experiments for evaluating the cellular structure of the explants. The explants were incubated (37 °C, 5% $CO_2$) for 24 h. Incubated explants were then divided for several analyses. 6 explants from the control and NPs treated (3 explants from each) were then fixed with 2% paraformaldehyde (PFA; Sigma) for 30 min at 4 °C.

### 2.4. Histological studies of the explants by light and TEM

A number of explants ($N = 6$) were processed for histological analysis. Specimens were fixed overnight in 4% PFA in 0.1 M phosphate buffer (pH 7.4), and rinsed in 0.1 M PBS. For TEM preparation and ultrastructural analysis specimens ($N = 12$) were osmicated, dehydrated in graded ethanols, embedded in Embed 812 epoxy resin (Electron Microscopy Sciences, Pennsylvania, USA) and poly-

**Table 1**
List of mouse primer sequences used in the study.

| Gene name | Acc. nr. | Forward primer | Reverse primer | Amplicon length |
|---|---|---|---|---|
| Ntrk1 (Trk A) | NM_001033124.1 | GCT TCT TTG GAG TCT GCA CC | TCA CCA CTA GTC CCT GAC CC | 273 bp |
| Ntrk2 (Trk B) | NM_008745.2 | CGG CAC ATA AAT TTC ACA CG | GTG AGG TTA GGA GCA GCC AG | 269 bp |
| Ntrk3 (Trk C) | NM_182809.2 | AAG TAA CCG GCT CAC CAC AC | GAT GCA GTA AAG GCT CTG GC | 166 bp |
| Ngfr (p75 NTR) | NM_033217.3 | CAA CCA GAC CGT GTG TGA AC | GAG AAC ACG AGT CCT GAG CC | 234 bp |

merized for 48 h at 60 °C, the specimens were processed according to manufacturers recommendation. 1 μm thick semithin sections were stained with toluidine blue for light microscopic evaluation and analysed under Zeiss Imager M1 microscope with Axio vision 4.6. 90 nm ultrathin sections were cut with a Leica UC6 microtome and transferred to hexagonal copper grids (Agar Scientific, England). Staining was performed using an automated system (Leica EM Stain) with uranyl acetate (5 g/L; 35 min) and lead citrate (5 g/L, 10 min) at 25 °C. The grids were examined with a Zeiss Libra 120 transmission electron microscope operating at 80 kV (Division of Ultrastructural Research and Evolutionary Biology, Institute of Zoology, Leopold Franzens University, Innsbruck, Austria).

### 2.5. Gene expression analysis in organotypic culture

Total RNA was isolated from P2 mouse cochleae ($N = 3$) and from organotypic cultures after 2 ($N = 3$), 4 ($N = 3$), and 24 ($N = 3$) h in culture. Total RNA was extracted by using 1 mL of PeqGold RNApure reagent from Peqlab (Erlangen, Germany), subsequently RNA was precipitated by isopropanol and glycogen (Genexpress, Wiener Neudorf, Austria) and washed with 75% ethanol (Tadros et al., 2008). Reverse transcription was completed using the "iScript cDNA Synthesis Kit" (Bio-Rad, Munich, Germany). Real-time quantitative PCR (qPCR) was performed using "iQ Sybr Green Supermix" (Bio-Rad) in a MyiQ cycler (Bio-Rad). Primers were designed by using the program Primer Blast of NCBI (NIH, Bethesda, MD, USA), primers sequences are summarized in Table 1. Based on our own experience and on relevant publications (Manji et al., 2006; Tadros et al., 2008) 18S rRNA was used as endogenous control. The primers for 18S rRNA are published (Haller et al., 2004). The relative gene expression was calculated by the dCq method: where relative expression is equal with $2^{-dCq}$, where −dCq is: $Cq_{18S} - Cq_{gene\ of\ interest}$. Cq: quantification cycle: the number of cycles where the detected bound Sybr Green fluorescence first emerges from the baseline (quantitative synthesis starts). All gene expression analyses were done in duplicate. In order to quantify the mRNA expression of genes of interest real-time RT-PCR was performed using the sequences shown in Table 1. Ntrk1, Ntrk2, Ntrk3 and Ngfr code for Trk A, Trk B, Trk C and p75 receptor, respectively.

### 2.6. Confocal microscopy for assessing cell specific targeting

The NPs incubated as well as control explants were washed 3 times with PBS. To identify cochlear hair cells explants were stained with phalloidine, binding selectively to F-actin that is expressed in high amount in hair cell stereocilia and cuticular plates. The specimens were permeabilized for 30 min with 0.3% Triton X-100, 1% BSA–PBS followed by incubation with Alexa 633 Phalloidin (Invitrogen, California, USA) (1:40 in PBS–1% BSA) for 30 min. The explants were washed 3 times with PBS and mounted in Vectashield with or without DAPI (Vector Laboratories, Szabo-Scandic, Vienna, Austria). Explants were analysed on a Zeiss LSM 510 META confocal laser scanning microscope with software release 3.2. Frame size was set as predefined number of pixels (512 × 512 pixels) and colour depth was set to 8 bit. Z-stacks through the explants were made with Zeiss PlanNeofluars 10×/0.3, 40×/1.3 and PlanApos 20/0.8 and 63×/1.4 using the 546, 633, 405 nm laser line of HeNe and diode lasers. Laser power was set to 63%, 65% and 5% for 546, 633, 405 nm, respectively. Confocal stacks were acquired in single-track unidirectional line scan mode using separate channels. A NTF 545 beamsplitter and 505–550 bandpass filter was used for Alexa 488/FITC detection, a 650 nm longpass filter for Alexa 633/cy5 and NTF 490 beamsplitter with 650 nm longpass filter for Qdot 655, respectively. Additionally the transmitted light channel was recorded to visualize gross tissue morphology. Pinholes were adjusted so that the optical section thickness of the immunofluorescent signals was equal; detector gain and amplifier offset were adjusted using the range indicator function of the Zeiss software. Amplifier gain was set to 1 and line scans were set to 4 times mean average with a scan speed of 1.6 μs pixel time.

### 2.7. Immunofluorescence with anti-Pan-Trk Ab and p75 on the cultured organotypic explants

Immunofluorescence staining was performed on the cultured P3 mice cochlea with chicken Anti-Pan-Trk Ab (G1581, Promega) and rabbit polyclonal anti-p75 antibody (a kind gift from Prof. Louis Reichardt, University of California, San Francisco). Briefly, explants were cultured for 24 h and fixed in 2% PFA in 0.1 M PBS for 30 min and washed 3 times in 0.1 M PBS. Unspecific binding sites were blocked for 2 h with two different solutions containing of 30% normal donkey serum (NDS), 0.3% of Triton X-100 in 0.1 M PBS for Anti-p75 Ab and 30% normal goat serum (NGS), 0.3% Triton in 0.1 M PBS for anti-Pan-Trk. The Pan-Trk antibody immunolabels all tyrosine kinase receptors (TrkA, TrkB, TrkC) and was raised against the cytoplasmic domain, corresponding to residues 778–790 of the carboxy terminus of TrkA, which is a conserved region of the trk receptor family (Pflug et al., 1995; Mischel et al., 2001; Miller et al., 2007). Specimens were incubated overnight at 4 °C in diluting solution containing 0.1 M PBS, 1% NDS, p75 (1:1000) and 0.1 M PBS, 1% NGS, Anti-Pan-Trk Ab (1:300). The explants then were incubated at room temperature for 2 h. Samples were then rinsed 5 times in 0.1 M PBS and immersed in a solution containing 1% NGS in 0.1 M PBS, Alexa 488 Goat Anti Chicken for Pan-Trk Ab and 1% NDS in 0.1 M PBS, Alexa 488 Donkey Anti Rabbit for p75 (1:2000) or Quantum Dot secondary conjugate Qdot 655 goat anti-rabbit F(ab′)2 (Invitrogen). Explants were incubated for 2 h at room temperature in a dark humid chamber and rinsed 3 times in 0.1 M PBS. Specimens were mounted on glass slides with Vectashield containing DAPI nuclear stain for fluorescence and confocal microscopy.

### 2.8. Analysis of targeting efficacy by PC12 cell culture

Cells were plated on rat tail collagen-1- (BD Biosciences, Bedford, MA, USA) coated Fluorodishes (World Precision Instruments,

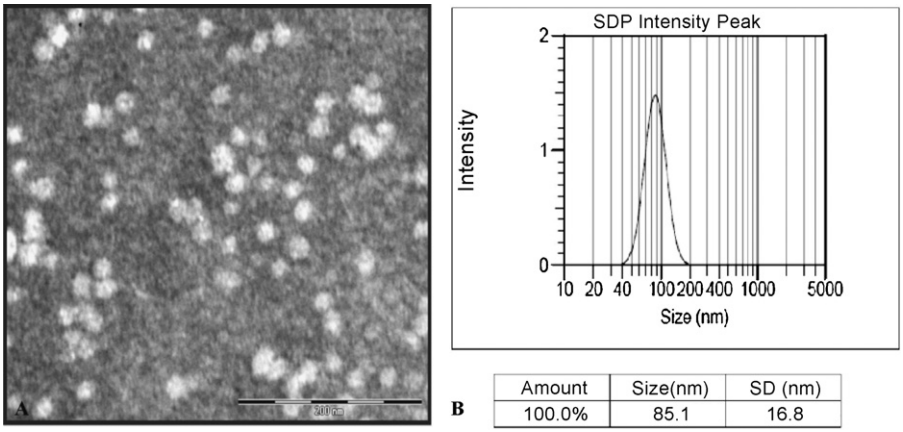


**Fig. 2.** (A) TEM image showing the spherical morphology of the polymersome nanoparticles negatively stained with uranyl acetate. (B) Example DLS result showing the typical nanoparticle size to be 85.1 (±) 16.8 nm.

Sarasota, FL, USA) at $10^5$/mL medium in Roswell Park Memorial Institute (RPMI) 1640 medium supplemented with 10% horse serum, 5% fetal calf serum, PSN 1% and 1% antibiotics (5 mg/mL penicillin, 5 mg/mL streptomycin, 10 mg/mL neomycin) as published before (Klimaschewski et al., 2006). Cells were subcultured every 3–4 days. 24 h after plating the media was replaced. Unfunctionalized, hNgf_EE conjugated, and random sequenced ligand of hNgf_EE conjugated NPs were added at 125 μg/mL and incubated for 20 h. After 20 h the medium was removed, cells were washed once with PBS, and fixed with freshly prepared 4% PFA in PBS for 15 min, washed in PBS and covered with MOWIOL (Roth, Karlsruhe, Germany). Subsequently Fluorodishes were observed by confocal microscopy.

## 3. Results and discussion

### 3.1. Preparation of polymersome nanoparticles

Degeneration of sensory hair cells and SGNs within the inner ear is one of the main causes of age related hearing loss (Gates and Mills, 2005). The ability to deliver therapeutic agents to these cells may form the basis of an effective treatment. However, drug delivery to the inner ear is problematic due to the compartmentalized nature of the organ. NPs have been frequently considered as vehicles for delivering chemotherapeutic agents to tumor cells (Malam et al., 2009). NPs are also desirable as delivery vehicles as drugs can be encapsulated within them and the surface can be functionalized with a variety of ligands that direct delivery to the desired cell population. In the current work we have investigated polymersome NPs as potential drug delivery vehicles to the SGNs within the inner ear.

TEM imaging shows a spherical structure of polymersomes (Fig. 2A). The negative stain permeates the hydrophilic corona of the nanoparticle and highlights the hydrophobic core. Size measurement by DLS showed a characteristic size of 85.1 (±) 16.8 nm for the unfunctionalized NPs (Fig. 2B). Analysis by DLS demonstrated the typical size of the hNgf_EE and scrambled hNgf_EE functionalized NPs to be to be 85.5 (±) 11.2 nm and 88.5 (±) 14.7 nm, respectively.

### 3.2. Toxicity analysis of nanoparticles in PC-12 cells

We found that at the higher concentration of NPs without ligand (25 μg/mL), 1.7% of cells were dead in contrast to 4.2% for NPs with ligand. The percentage of dead cells in untreated control experiment was 2.14%. These values indicate the absence of any toxic effect both by NPs with and without ligand (under 5%).

We analysed the percentage of PI-positive cells in the attached population by direct microscopical evaluation; we did not find differences between the samples with particles carrying the ligand and particles without it. Indeed, the cell morphology appeared normal, without signs of cell detachment, or nuclear fragmentation exceeding the basal range. This was confirmed over the whole range of NP concentrations explored (Fig. 3).

### 3.3. Histology of mice inner ear organotypic cultures: a good model for nanoparticle based cell specific targeting

Semithin sections and ultrastructural TEM imaging of the cultured explants have shown unimpaired morphology after 24 h in culture, with well preserved inner hair cells (IHCs) and outer hair cells (OHCs) in the immature sensory epithelium (Fig. 4A). Neurons in the spiral ganglion (Fig. 4B) appeared to be morphologically intact as confirmed by TEM (Fig. 4C). Organotypic cochlear explants represent a complex multi-cellular *ex vivo* environment with the potential to assess biological function (Bertolaso et al., 2003; Qi et al., 2008). Tissue structure did not show any marked difference from a dissected and immediately fixed inner ear (not shown). Explants incubated with scrambled hNgf_EE conjugated NPs (Fig. 4D) and targeted NPs (Fig. 4E and F) also did not show any morphological deviations from control tissue.

We could not visualize NPs in cells of the inner ear at TEM level. Single NPs are extremely difficult to distinguish from cellular organelles. To chase NPs at lower concentrations a tag such as gold or iron oxide would be very important. Further investigations are going on to incorporate gold or iron oxide to the polymersome NPs.

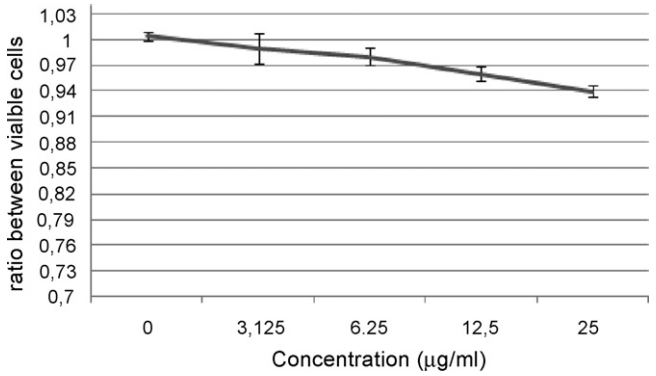


**Fig. 3.** Cell viability after NPs treatment on PC12 cells. The graph shows the ratio (±s.d.) between viable cells in samples treated with NPs functionalized with hNgf_EE or scrambled hNgf_EE peptides. In abscissa is indicated the ratio and in ordinate the treatment concentrations.

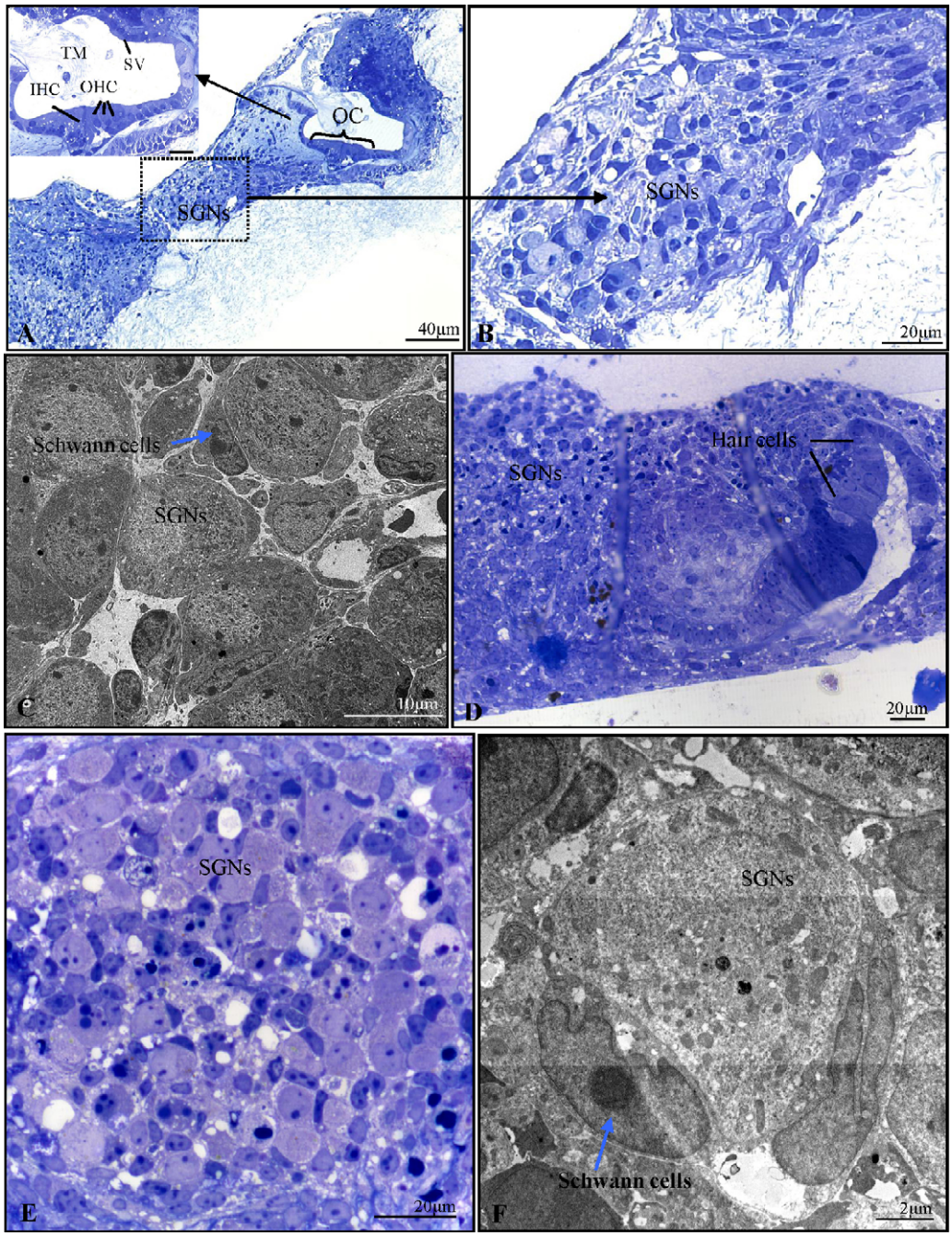


**Fig. 4.** Histology of mice inner ear organotypic cultures. (A and B) Semithin section of the 24 h cultured explant shows a good structure of the organ of Corti and spiral ganglion cells, OC = organ of Corti, IHC = inner hair cell, OHC = outer hair cell, TM = Tectorial membrane and SGNs = spiral ganglion neurons. (C) Electron micrograph of the 24 h cultured cochlear explant shows non-toxicity to the spiral ganglion neurons and to the Schwann cells. (D) Semithin section indicates unchanged morphology of the spiral ganglion neurons. Hair cells of the explant, which were incubated with scrambled hNgf_EE-NPs. (E) After 24 h of hNgf_EE-NP incubation, the spiral ganglion neurons and the Schwann cells of the explant shows unimpaired structure. (F) The TEM image presents the ultrastructure of the 24 h hNgf_EE-NPs incubated spiral ganglion neurons and Schwann cells, which confirms the structural integrity.

This culture model allowed us to develop functional screening of different multifunctional nanoparticles, in which the outcome may be comparable with the in vivo condition (Sundstrom et al., 2005).

### 3.4. Analysis of Trk receptor and p75 expression in organotypic culture by RT-PCR

Neurotrophins are responsible for regulating the fate of neural precursors, axonal and dendritic growth, patterning, expression and activity of functionally important proteins, including ion channels and neurotransmitter receptors (Huang and Reichardt, 2003). The Trks are a family of three tyrosine kinase receptors Trk A, B, and C. In neurons the neurotrophin-bound Trk receptors are internalized by endocytosis and transported back to the cell body in endosomes where they can activate signal transduction pathways involved in neuronal survival (Watson et al., 2001). Trks and p75 have a major role during development particularly during the critical period of rearrangement of neural connections (Knipper et al., 1996). Application of exogenous neurotrophic factors can enhance the survival efficiency of SGNs and also can induce the re-growth of SGN peripheral processes (Glueckert et al., 2008). Co-expression

of the Trks and p75 receptors and their ligands has been proposed to be functionally involved in regulating the survival of neurons. Trk receptors are also believed to contribute to tumorigenicity and metastasis in humans (Desmet and Peeper, 2006). That is why a localized and targeted drug delivery with NPs may be advantageous compared to conventional neurotrophin application with an even distribution. This may prevent possible leakage via cerebrospinal fluid to the brain.

In order to quantify the mRNA expression of Trks and p75 receptor real-time RT-PCR was performed using the primer sequences shown in Table 1. ntrk1, ntrk2, ntrk3 and ngfr are the gene names for Trk A, Trk B, Trk C and p75 receptor, respectively. The aim of this analysis was to assess the target availability of ntrk1, ntrk2, ntrk3 and ngfr during the period of organotypic culturing.

Total RNA was isolated and reverse transcribed at 0, 2, 4 and 24 h from the organotypic culture. According to Manji et al. (2006) and Tadros et al. (2008) 18S rRNA was used as endogenous loading control. The Cq values (quantification cycle) of Sybr Green real-time qPCR of 18S rRNA were between 20 and 33. The Cq values of ntrk2 (Trk B), ntrk3 (Trk C) and ngfr (p75) were by 39–48. The gene expression analysis of ntrk2 (Trk B) did not show any amplification at early time points (0 and 2 h) of culture. In case of ntrk3 (Trk C) and ngfr (p75) time kinetics of the mRNA expression was investigated (Fig. 5A and B). The expression levels of both genes were decreased after 2 h of organotypic culturing compared to 0 h ($p = 0.009$ for ntrk3 (Trk C) and 0.0156 for nfgr (p75)). Between 2 and 24 h there was no significant change of gene expression of ntrk3 (Trk C) ($p = 0.472$) and of ngfr (p75) ($p = 0.365$) (Fig. 5A and B). NPs were added to the culture after 4 h in culture and were incubated till 24 h. Gene expression levels of ntrk2 (Trk B), ntrk3 (Trk C) and ngfr (p75) at 4 and 24 h of organotypic culture were compared and shown in Fig. 5C. At both 4 and 24 h ngfr (p 75) showed highest expression level, while ntrk2 (Trk B) was the lowest. At 24 h the expression levels of ntrk2 (Trk B), ntrk3 (Trk C) and ngfr (p75) did not change significantly compared to the levels after 4 h as tested by one-way ANOVA ($p = 0.09$) (Fig. 5C). Ntrk1 (Trk A) did not show detectable expression (no PCR amplification was observed) during the whole culture period. These data indicate that organotypic culture provides a stable target availability of Trks and p75 receptor during the 4–24 h of culture period.

### 3.5. Analysis of nanoparticle uptake in organotypic culture by confocal imaging

We found an equal distribution of NP fluorescent signal with non-conjugated NP samples. All cell types of the explant tissue showed uptake within the cytoplasm, intercellular spaces and extracellular matrix but NPs did not enter into the cell nucleus (Fig. 6A). The hair cells were highlighted with phalloidin in order to detect any toxic effect to these rather vulnerable sensory cells. We did not see any hair cell loss which is a well established indicator for ototoxicity (Ding et al., 2007).

Organotypic cultures incubated with hNgf_EE functionalized NPs showed higher uptake at the region of SGNs. After 12 h of NP exposure a dotted accumulation of the DiI signal was more intense and fluorescence signal was observed throughout the nerve fibers and to the hair cells (Fig. 6B). The targeting was more prominent after longer incubation for 24 h. High uptake was observed within SGNs and Schwann cells and nerve fibers and comparatively less DiI signal was detected in the hair cells. An even more intense signal was found in small cells of the spiral canal that may represent the Schwann cells (Fig. 6C, inset). No apparent hair cell loss was found (Fig. 6C).

Uptake of the NPs was mostly present in the cytoplasm and not found in nucleus (Fig. 6D). Uncontrolled penetration through the nuclear membrane might cause toxicity by DNA damage.

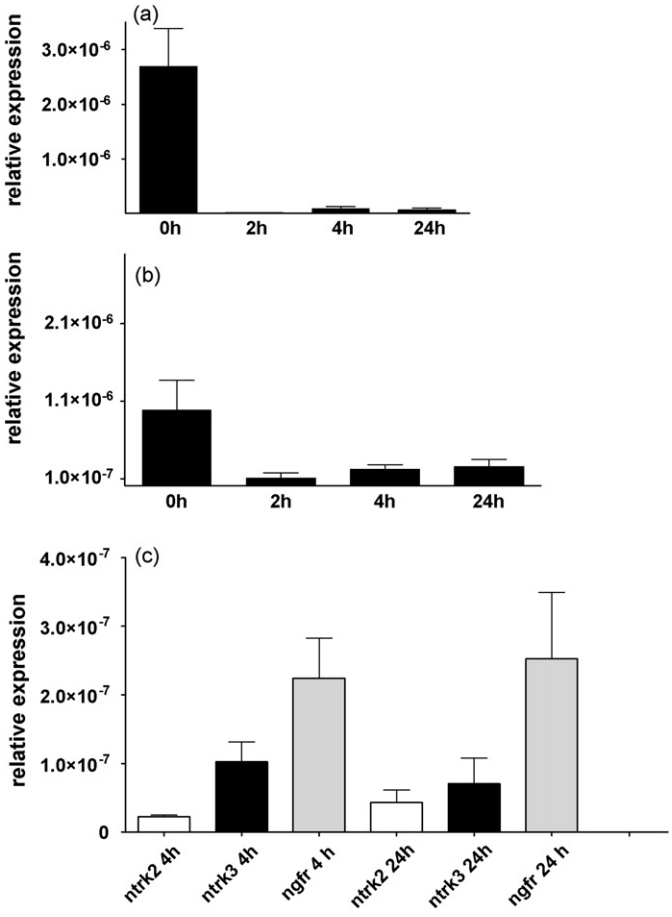


**Fig. 5.** Gene expression analysis of *ntrk* and *ngfr* genes in organotypic culture. A. Time kinetics of *ntrk3* gene expression in organotypic culture. Relative expression was calculated as described in Section 2. At 2 h a significant loss of gene expression is detected compared to 0 h ($p = 0.01$ by one-way ANOVA). Nevertheless, between 2 and 24 h no significant changes take place ($p = 0.472$ by one-way ANOVA). (B) Time kinetics of *ngfr* gene expression in organotypic culture. At 2 h a significant loss of gene expression is detected compared to 0 h ($p = 0.015$ by one-way ANOVA). Nevertheless, between 2 and 24 h no significant changes take place ($p = 0.365$ by one-way ANOVA). (C) Comparison of *ntrk 2-3* and *ngfr* gene expression at 4 and at 24 h. At both 4 and 24 h ngfr showed highest expression level, while ntrk2 was the lowest. At 24 h the expression levels of ntrk2-3 and ngfr did not change significantly compared to the levels at 4 h as tested by one-way ANOVA ($p = 0.09$).

Unspecific and less uptake was found by NPs with scrambled hNgf_EE compared to unfunctionalized and hNgf_EE ligand-conjugated NPs (Fig. 6E and F). In the lower magnified views scrambled NP exposed specimens (Fig. 6F) resembled results from the non-functionalized NPs. The spotty distribution of the scrambled hNgf_EE-NPs (Fig. 6E) may indicate that they remain within the endosome. In general the cellular uptake of NPs is accomplished by endocytosis followed by early endosome formation. The early endosomes mature into late endosomes and finally fuse with lysosomes, where pH drops down significantly and could degrade the NPs. Here we did not focus on the dynamics of endosomal vesicle formation and its fusion with the lysosomes. NP trafficking requires additional tools and has not been further evaluated here (Ding et al., 2007; Nam et al., 2009). There would be two possibilities for a successful release of the cargo from the NPs: (1) NPs may remain within the endosome but the drug finds the way into cytoplasm (Rosenholm et al., 2009); (2) NPs may escape from the endosome and can release the drug into the cytosol. It appears that NPs with scrambled hNgf_EE could not escape from the endosomal vesicles, hence shows spotty distribution.

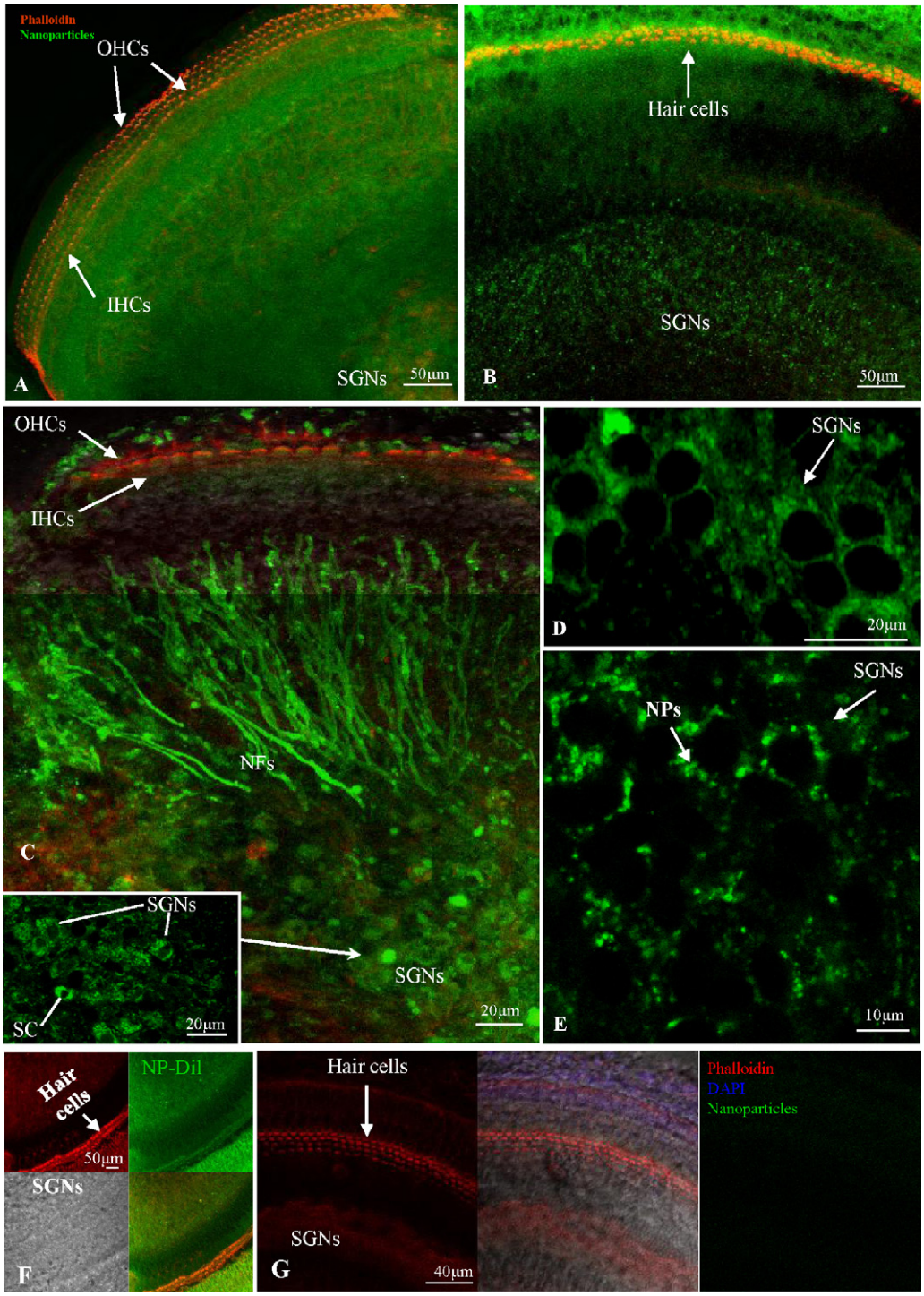


**Fig. 6.** Studies of nanoparticle uptake in organotypic culture by confocal imaging. (A) The confocal image showing uptake as well as intercellular penetration of NPs in the inner hair cells, outer hair cells, spiral ganglion neurons and to the cells of stria vascularis. IHCs = inner hair cells, OHCs = outer hair cells, SGNs = spiral ganglion neurons and SV = stria vascularies. (B) High amount of selective targeting by the hNgf_EE conjugated NPs, could be visualized at the region of spiral ganglion neurons of the explant, which is incubated for 12 h. Uptake was very high at stria vascularis and in hair cells. (C) Projection of the confocal images indicates cell-specific targeting by hNgf_EE functionalized nanoparticles at spiral ganglion neurons, Schwann cells (high magnification in the inset), nerve fibers and to the organ of Corti cells. Green fluorescence is for nanoparticles and blue fluorescence is for nuclear staining DAPI. (D) Highly magnified confocal image of spiral ganglion neurons are indicating specific binding of NPs functionalized with hNgf_EE. Even fluorescence signal indicates the release of Dil from the nanoparticles. (E) Confocal images for the nanoparticles functionalized with scrambled hNgf_EE shows spotty distribution of Dil in the cytoplasm of the spiral ganglion neurons. The uptaken nanoparticles seem to remain in vesicles of the spiral ganglion neurons. (F) Overview of the 24 h cultured explant shows unspecific binding by the scrambled hNgf_EE-NPs throughout the different cell populations of the cochlea. (G) Negative control explant without incorporation of nanoparticles shows no autofluorescence. Red = Phalloidin, no green fluorescence is visible. (For interpretation of the references to colour in this figure legend, the reader is referred to the web version of the article.)

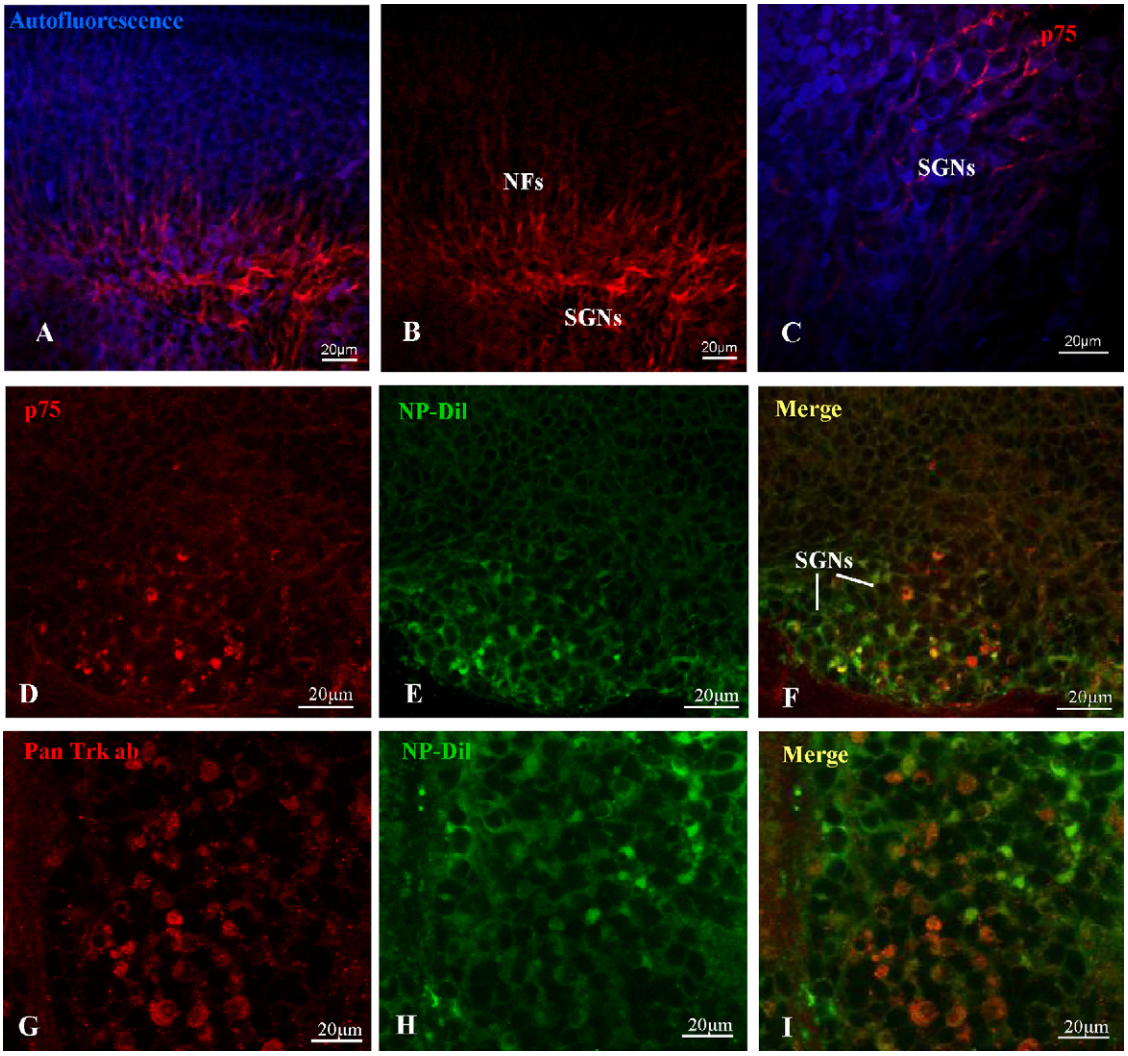


**Fig. 7.** Analysis of Trk receptor and p75 expression in organotypic culture by Immunofluorescence. (A and B) It represents p75 immunostaining along the nerve fibers and to the Schwann cells, less staining was found to the spiral ganglion neurons. NFs – nerve fibers, SGNs – spiral ganglion neurons. (C) Immediately fixed P-3 explant shows immunostaining by the Qdots for p75 in the Schwann cells and to the nerve fibers. (D) Confocal image clearly indicates localization of immunoreactivity for p75 in the spiral ganglion neurons and in the small cells (Schwann cells) (red). (E) Image shows nanoparticle targeting (green) mainly in the smaller cell populations and in the spiral ganglion neurons. We found a gradient in NP uptake and highly specific binding at the region of SGNs. F. Merged (yellow) confocal image represents colocalization of p75 (red) as well as the nanoparticles (green) (functionalized with hNgf_EE) mainly in the small cells and also binding can be found to the spiral ganglion neurons. Confocal image of the 24 h hNgf_EE-NP incubated explant showing Anti Pan-Trk (red) (G) immunostaining as well as nanoparticle (green) (H) binding to the spiral ganglion neurons and to the small cells (Schwann cells). (I) Merged (yellow) confocal image shows colocalization of Anti-Pan-Trk Ab immunostaining (red) with nanoparticles (green), functionalized with hNgf_EE, mainly in the Smaller cells surrounding to spiral ganglion neurons. Colocalization was found also in spiral ganglion neurons but in less amount. (For interpretation of the references to colour in this figure legend, the reader is referred to the web version of the article.)

As hNgf_EE has the specific targeting ability to the Trks and p75 receptors, it can be contemplated that hNgf_EE conjugated NPs were uptaken by the receptor-mediated pathway. This may have an influence in the endosomal escape. Further experiments will be performed by incorporating different drugs into the NPs and the biological effect will be studied.

In control experiments (Fig. 7G) shows a confocal image of three rows of outer hair cells and one row of inner hair cells that is congruent with the normal mosaic pattern of hair cell distribution in the reticular lamina confirming no obvious toxicity or unspecific fluorescent signal.

### 3.6. *Analysis of Trk receptor and p75 expression in organotypic culture by immunofluorescence*

Fig. 7A–C (dissected and immediately stained) shows immunoreactivity for p75 along nerve fibers and around SGNs. This indicates presence of p75 receptor in Schwann cells surrounding SGNs and nerve fibers as far as the habenula perforata. Nerve fibers lose the Schwann cell sheath as they enter the sensory epithelium. The staining pattern of p75 is similar to the targeted NP binding (can be compared with Fig. 6C).

After culturing the explant for 24 h in the presence of hNgf_EE-NPs, p75 immunostaining shows more differential expression again in the small cells of the SGN region (Fig. 7D). We could find selective binding of hNgf_EE-NPs at the region of SGN (Fig. 7E). Interestingly we found colocalization of Dil signal and p75 immunoreactivity mainly in small cells of the SGN region. These cells situated in between the bigger neurons likely represent the Schwann cells, which showed very high uptake of NPs and high expression of p75 (Fig. 7F).

We could find differences in the expression pattern of p75 and Trk receptors in the SGNs. Anti-Pan-Trk staining showed spotted distribution within the whole soma of the SGNs (Fig. 7G) but intensity of NP uptake is higher in small cells (Fig. 7H) that show no or very less immunostaining for Trk receptors. Merge image (Fig. 7I)

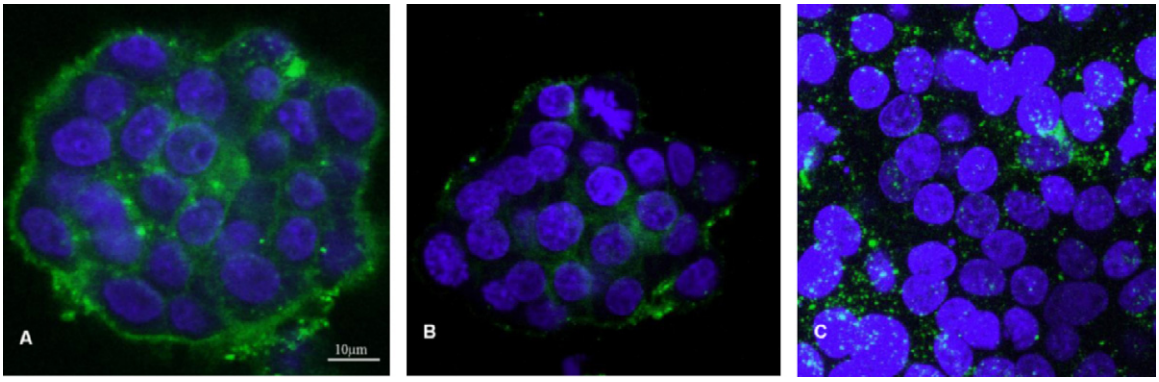


**Fig. 8.** Analysis of nanoparticle uptake, Trk receptor and p75 expression in PC-12 cells. (A) PC-12 cells incubated with nanoparticles without any surface functionalization; confocal image shows high unspecific cellular uptake. Green and blue fluorescence corresponds nanoparticles and nuclear staining with DAPI, respectively. (B) Confocal image (projection) indicates a very low level of nanoparticles (functionalized with hNgf_EE, green fluorescence) uptake. Blue fluorescence is DAPI. (C) Projected confocal image shows clustered unspecific uptake of the nanoparticles (functionalized with scrambled hNgf_EE). Green fluorescence is for nanoparticles and blue is for DAPI. (For interpretation of the references to colour in this figure legend, the reader is referred to the web version of the article.)

shows the overlapping between the Trk expressions and NP targeting. We presume that the Schwann cells facilitate the NPs uptake to the Spiral ganglion cells by means of intercellular transport. We think that the hNgf_EE conjugated NPs could target the Trks and p75 receptors. These would help to understand the NP-hNgf_EE based receptor targeting and receptor-mediated NP internalization in the SGNs.

### *3.7. Analysis of nanoparticle uptake, Trk receptor and p75 expression in PC-12 cells*

The targetability of unfunctionalized, hNgf_EE and scrambled peptide-conjugated nanoparticles were analysed in PC-12 cells. We evaluated the expression level of Trk A, B, C and p75 by RT-PCR and could confirm previously published work (Urdiales et al., 1998; Bilderback et al., 1999; Rosenholm et al., 2009). Expression of Trk A was confirmed, and a low level of p75 was found (data not shown). Unfunctionalized NPs showed high, non-specific uptake into the cytoplasm (Fig. 8A). Very few uptake was found with hngf_EE functionalized NPs (Fig. 8B). Spotty uptake was found surrounding the cells which were incubated with scrambled hNgf_EE conjugated NPs (Fig. 8C). Unfunctionalized nanoparticles may not be dependant to the receptor-mediated internalization; hence it showed high level of uptake to the cells. Lower level of Trk A and p75 expression minimizes the uptake of functionalized targeted NPs, which are evenly distributed. Scrambled hNgf_EE-NPs showed similar spotty uptake, which was also detected in the SGNs. It raises a great interest to understand the mechanism of pathways involved in receptor and nonreceptor-mediated NP uptake and its trafficking within the neuronal cells of the inner ear.

## 4. Conclusion

Our results indicate that organotypic culture represents a relevant cochlea model regarding tissue structure and gene expression. Polymersome nanoparticles either functionalized or not did not show any obvious signs of toxicity in both organotypic culture and PC-12 cells. We have shown that polymersome nanoparticles functionalized with the hNgf_EE peptide have a great potential for a specific cell targeting to SGNs in cochlear organotypic explant cultures. Compared to polymersomes functionalized with a scrambled hNgf_EE sequence or no peptide there is a marked increase in specificity toward SGNs. We have also shown that the expression levels of Trks and p75 do not significantly change over the time course of the experiment.

We do not yet know the precise mechanism in which the hNgf_EE functionalized polymersomes are taken up via receptor-mediated interaction with Trk receptors. Future work will be done to explore the potential of these hNgf_EE functionalized polymersomes, both to investigate the mechanism of uptake as well as the effects of delivering a therapeutic agent.

## Acknowledgements

Our work was supported by European Community; Grant number: NMP4-CT-2006-026556 Integrated EU project and Austrian Science Foundation (FWF) P15948-B05. We would like to express our thanks to Prof. Louis Reichardt, University of California, San Francisco for his kind gift of the anti-p75 antibody. We also thank Prof. Elisabeth Bock, Prof. Vladimir Berezin and Christina Fobian for proving us with useful information regarding hNgf_EE. We are grateful to Dr. Barbara Hausott for providing PC12 cell lines and culture protocols. All surgical, experimental, and euthanasia procedures were carried out in accordance with all regulations mandated by the Austrian Ministry of Animal Welfare as well as to laws stipulated by the Declarations of Helsinki.

## References

Bertolaso, L., Bindini, D., Previati, M., Falgione, D., Lanzoni, I., Parmeggiani, A., Vitali, C., Corbacella, E., Capitani, S., Martini, A., 2003. Gentamicin-induced cytotoxicity involves protein kinase C activation, glutathione extrusion and malondialdehyde production in an immortalized cell line from the organ of corti. Audiol. Neurootol. 8, 38–48.

Bilderback, T.R., Gazula, V.R., Lisanti, M.P., Dobrowsky, R.T., 1999. Caveolin interacts with Trk A and p75(NTR) and regulates neurotrophin signaling pathways. J. Biol. Chem. 274, 257–263.

Christian, N.A., Milone, M.C., Ranka, S.S., Li, G., Frail, P.R., Davis, K.P., Bates, F.S., Therien, M.J., Ghoroghchian, P.P., June, C.H., Hammer, D.A., 2007. Tat-functionalized near-infrared emissive polymersomes for dendritic cell labeling. Bioconjug. Chem. 18, 31–40.

Desmet, C.J., Peeper, D.S., 2006. The neurotrophic receptor TrkB: a drug target in anti-cancer therapy? Cell. Mol. Life Sci. 63, 755–759.

Ding, D., Jiang, H., Wang, P., Salvi, R., 2007. Cell death after co-administration of cisplatin and ethacrynic acid. Hear. Res. 226, 129–139.

Discher, B.M., Won, Y.Y., Ege, D.S., Lee, J.C., Bates, F.S., Discher, D.E., Hammer, D.A., 1999. Polymersomes: tough vesicles made from diblock copolymers. Science 284, 1143–1146.

Farokhzad, O.C., Cheng, J., Teply, B.A., Sherifi, I., Jon, S., Kantoff, P.W., Richie, J.P., Langer, R., 2006a. Targeted nanoparticle-aptamer bioconjugates for cancer chemotherapy in vivo. Proc. Natl. Acad. Sci. U.S.A. 103, 6315–6320.

Farokhzad, O.C., Karp, J.M., Langer, R., 2006b. Nanoparticle-aptamer bioconjugates for cancer targeting. Expert Opin. Drug Deliv. 3, 311–324.

Farokhzad, O.C., Langer, R., 2006. Nanomedicine: developing smarter therapeutic and diagnostic modalities. Adv. Drug Deliv. Rev. 58, 1456–1459.

Fritzsch, B., Beisel, K.W., Hansen, L.A., 2006. The molecular basis of neurosensory cell formation in ear development: a blueprint for hair cell and sensory neuron regeneration? Bioessays 28, 1181–1193.

Fritzsch, B., Silos-Santiago, I., Bianchi, L.M., Farinas, I., 1997. The role of neurotrophic factors in regulating the development of inner ear innervation. Trends Neurosci. 20, 159–164.
Gates, G.A., Mills, J.H., 2005. Presbycusis. Lancet 366, 1111–1120.
Gelperina, S., Kisich, K., Iseman, M.D., Heifets, L., 2005. The potential advantages of nanoparticle drug delivery systems in chemotherapy of tuberculosis. Am. J. Respir. Crit. Care Med. 172, 1487–1490.
Glueckert, R., Bitsche, M., Miller, J.M., Zhu, Y., Prieskorn, D.M., Altschuler, R.A., Schrott-Fischer, A., 2008. Deafferentation-associated changes in afferent and efferent processes in the guinea pig cochlea and afferent regeneration with chronic intrascalar brain-derived neurotrophic factor and acidic fibroblast growth factor. J. Comp. Neurol. 507, 1602–1621.
Haller, F., Kulle, B., Schwager, S., Gunawan, B., von Heydebreck, A., Sultmann, H., Fuzesi, L., 2004. Equivalence test in quantitative reverse transcription polymerase chain reaction: confirmation of reference genes suitable for normalization. Anal. Biochem. 335, 1–9.
He, X.L., Garcia, K.C., 2004. Structure of nerve growth factor complexed with the shared neurotrophin receptor p75. Science 304, 870–875.
Huang, E.J., Reichardt, L.F., 2001. Neurotrophins: roles in neuronal development and function. Annu. Rev. Neurosci. 24, 677–736.
Huang, E.J., Reichardt, L.F., 2003. Trk receptors: roles in neuronal signal transduction. Annu. Rev. Biochem. 72, 609–642.
Kaplan, D.R., Miller, F.D., 1997. Signal transduction by the neurotrophin receptors. Curr. Opin. Cell Biol. 9, 213–221.
Kaplan, D.R., Miller, F.D., 2000. Neurotrophin signal transduction in the nervous system. Curr. Opin. Neurobiol. 10, 381–391.
Klimaschewski, L., Hausott, B., Ingorokva, S., Pfaller, K., 2006. Constitutively expressed catalytic proteasomal subunits are up-regulated during neuronal differentiation and required for axon initiation, elongation and maintenance. J. Neurochem. 96, 1708–1717.
Knipper, M., Zimmermann, U., Rohbock, K., Kopschall, I., Zenner, H.P., 1996. Expression of neurotrophin receptor trkB in rat cochlear hair cells at time of rearrangement of innervation. Cell Tissue Res. 283, 339–353.
Letchford, K., Burt, H., 2007. A review of the formation and classification of amphiphilic block copolymer nanoparticulate structures: micelles, nanospheres, nanocapsules and polymersomes. Eur. J. Pharm. Biopharm. 65, 259–269.
Lin, J.J., Ghoroghchian, P.P., Zhang, Y., Hammer, D.A., 2006. Adhesion of antibody-functionalized polymersomes. Langmuir 22, 3975–3979.
Lindgren, M., Hallbrink, M., Prochiantz, A., Langel, U., 2000. Cell-penetrating peptides. Trends Pharmacol. Sci. 21, 99–103.
Malam, Y., Loizidou, M., Seifalian, A.M., 2009. Liposomes and nanoparticles: nanosized vehicles for drug delivery in cancer. Trends Pharmacol. Sci. 30, 592–599.
Manji, S.S., Sorensen, B.S., Klockars, T., Lam, T., Hutchison, W., Dahl, H.H., 2006. Molecular characterization and expression of maternally expressed gene 3 (Meg3/Gtl2) RNA in the mouse inner ear. J. Neurosci. Res. 83, 181–190.
Miller, J.M., Le Prell, C.G., Prieskorn, D.M., Wys, N.L., Altschuler, R.A., 2007. Delayed neurotrophin treatment following deafness rescues spiral ganglion cells from death and promotes regrowth of auditory nerve peripheral processes: effects of brain-derived neurotrophic factor and fibroblast growth factor. J. Neurosci. Res. 85, 1959–1969.
Mischel, P.S., Smith, S.G., Vining, E.R., Valletta, J.S., Mobley, W.C., Reichardt, L.F., 2001. The extracellular domain of p75NTR is necessary to inhibit neurotrophin-3 signaling through TrkA. J. Biol. Chem. 276, 11294–11301.
Mukherjee, S., Ghosh, R.N., Maxfield, F.R., 1997. Endocytosis. Physiol. Rev. 77, 759–803.
Nam, H.Y., Kwon, S.M., Chung, H., Lee, S.Y., Kwon, S.H., Jeon, H., Kim, Y., Park, J.H., Kim, J., Her, S., Oh, Y.K., Kwon, I.C., Kim, K., Jeong, S.Y., 2009. Cellular uptake mechanism and intracellular fate of hydrophobically modified glycol chitosan nanoparticles. J. Control. Release 135, 259–267.
Pflug, B.R., Dionne, C., Kaplan, D.R., Lynch, J., Djakiew, D., 1995. Expression of a Trk high affinity nerve growth factor receptor in the human prostate. Endocrinology 136, 262–268.
Qi, W., Ding, D., Salvi, R.J., 2008. Cytotoxic effects of dimethyl sulphoxide (DMSO) on cochlear organotypic cultures. Hear. Res. 236, 52–60.
Reichardt, L.F., 2006. Neurotrophin-regulated signalling pathways. Philos. Trans. R. Soc. Lond. B: Biol. Sci. 361, 1545–1564.
Rosenholm, J.M., Meinander, A., Peuhu, E., Niemi, R., Eriksson, J.E., Sahlgren, C., Linden, M., 2009. Targeting of porous hybrid silica nanoparticles to cancer cells. ACS Nano 3, 197–206.
Sundstrom, L., Morrison III, B., Bradley, M., Pringle, A., 2005. Organotypic cultures as tools for functional screening in the CNS. Drug Discov. Today 10, 993–1000.
Tadros, S.F., D'Souza, M., Zhu, X., Frisina, R.D., 2008. Apoptosis-related genes change their expression with age and hearing loss in the mouse cochlea. Apoptosis 13, 1303–1321.
Urdiales, J.L., Becker, E., Andrieu, M., Thomas, A., Jullien, J., van Grunsven, L.A., Menut, S., Evan, G.I., Martin-Zanca, D., Rudkin, B.B., 1998. Cell cycle phase-specific surface expression of nerve growth factor receptors TrkA and p75(NTR). J. Neurosci. 18, 6767–6775.
Watson, F.L., Heerssen, H.M., Bhattacharyya, A., Klesse, L., Lin, M.Z., Segal, R.A., 2001. Neurotrophins use the Erk5 pathway to mediate a retrograde survival response. Nat. Neurosci. 4, 981–988.